# Quantum crystals in a trapped Rydberg-dressed Bose-Einstein condensate

C.-H. Hsueh,[1] T.-C. Lin,[2] T.-L. Horng,[3] and W. C. Wu[1]

[1]*Department of Physics, National Taiwan Normal University, Taipei 11677, Taiwan*
[2]*Department of Mathematics, National Taiwan University, Taipei, 10617, Taiwan*
[3]*Department of Applied Mathematics, Feng Chia University, Taichung 40724, Taiwan*

Based on a mean-field approach, spontaneously crystalline ground states, called quantum crystals, of a trapped Rydberg-dressed Bose-Einstein condensate are numerically investigated. In a quasi-two-dimensional geometry, a hexagonal lattice of condensate droplets manifests when dressed coupling is above a critical value. The onset of the crystallized state is characterized by a drastic drop of the nonclassical rotational inertia fraction (NCRIF). Nevertheless, the NCRIF remains a large value for a large span of dressed coupling, which indicates that the long-range phase coherence of a superfluid is preserved in the crystallized state. By relaxing the confinement against the two-dimensional geometry and by introducing an anisotropic interaction, an $AB$ stacking bilayer lattice and a nearly square lattice, respectively, are also available in the system. A quasi-one-dimensional lattice is also shown.

## I. INTRODUCTION

Superfluidity, which implies a long-range phase coherence, is a crucial property at low temperatures of many quantum liquids or gases such as liquid helium or Bose-Einstein condensates (BECs), whereas crystallization implies a long-range configurational order. Superfluidity and crystallization are generally two conflicting properties. Penrose and Onsager [1] were the first to consider a BEC in a solid and concluded that such a *supersolid* state simultaneously possessing crystalline and superfluid properties was impossible. Since then, this question has been revisited by a number of authors [2–4] and has been a matter of much speculation for the past 40 years. Recently, the observation of a supersolid phase in ⁴He systems [5] revitalized this fundamental interest.

An alternative and excellent candidate in which to study supersolidity is atomic BECs, which provide a clean and experimentally controllable system. The crystal structure in solid helium can be replaced by the modulated density in a BEC. Density modulated BECs are already formed by the imposition of an external potential, creating the so-called optical lattices. In these systems, by varying the properties of the optical lattice, the condensate was shown to exhibit a Mott insulator-superfluid phase transition [6–9]. More recently, it has been shown that supersolidity might be present for Rydberg atoms in the dipole–van der Waals (vdW) blockade regime [10–13]. Cinti *et al.* [11] considered a dipole-dipole interaction softening at short distance, allowing for a ground-state computation that happens to display the properties of supersolidity. It proved that a quantum system of interacting particles can exhibit both a crystalline structure and a superfluidity property. Similar results were obtained by Saccani *et al.* [12] by using a Heaviside-function interaction. Based on a mean-field treatment, Henkel *et al.* [13] proposed that a BEC of particles interacting through an isotropically repulsive vdW interaction with a softened core might support a density modulation. They found that the Fourier transform of such an interaction has a partial attraction in momentum

space, which gives rise to a transition from a homogeneous BEC to a supersolid phase because of the roton instability (see also Refs. [14,15]).

Based on the mean-field Gross-Pitaevskii (GP) treatment, this paper attempts to study the ground-state density distribution of a trapped Rydberg-dressed BEC. By comparing to other GP work that did not consider the effect of trapping [13], we exactly solve the nonlocal GP equation with a trap. In a quasi-two-dimensional (quasi-2D) geometry, it is shown that periodic structures of a Rydberg-dressed BEC can undergo a transition from concentric rings to a lattice (or crystalline) if the long-range dressed interaction coupling $\alpha$ is above a certain critical value. The lattices are formed in terms of crystalline condensate droplets, called quantum crystals, whose onset is characterized by a drastic drop of the nonclassical rotational inertia fraction (NCRIF) proposed by Leggett [4]. Nevertheless, the NCRIF, which stands for the superfluid fraction, remains at large values for a large span of $\alpha$ and supports that the crystalized state is indeed a supersolid state. The quasi-2D crystalline structure is a hexagonal lattice, which can turn into a nearly square lattice if the interaction acquires an anisotropic component in the presence of an external electric field (Stark effect). Moreover, a multilayer crystal structure such as an $AB$ stacking bilayer is also possible when the frozen axis is relaxed or the particle number is increased.

The paper is organized as follows. In Sec. II we outline the mean-field treatment of the nonlocal GP equation for studying ground states of the Rydberg-dressed Bose-condensed system. A crystalized state of the condensate droplet is shown to exhibit in a quasi-2D geometry that is accompanied by a drastic drop of the NCRIF. Section III shows more crystal structures available in the system, such as those obtained by relaxing the confinement against the quasi-2D geometry of a bilayer structure and by introducing an anisotropic interaction in a nearly square lattice. The crystalline structure in the case of a quasi-1D geometry is also presented. We summarize in Sec. IV.

## II. MEAN-FIELD TREATMENT

We start from a nonlocal mean-field Gross-Pitaevskii equation

$$i\hbar\partial_t\Psi(\mathbf{r},t) = \left[-\frac{\hbar^2\nabla^2}{2M} + V_{\text{ext}}(\mathbf{r}) + g|\Psi(\mathbf{r},t)|^2 \right.$$
$$\left. + \int U\left(\mathbf{r}-\mathbf{r}'\right)|\Psi(\mathbf{r}',t)|^2 d\mathbf{r}'\right]\Psi(\mathbf{r},t), \quad (1)$$

where

$$U(\mathbf{r}-\mathbf{r}') = \frac{\tilde{C}_6}{R_c^6 + |\mathbf{r}-\mathbf{r}'|^6} \quad (2)$$

is the isotropically repulsive, long-range vdW interaction between Rydberg-dressed ground-state atoms [16,17]. Here $\tilde{C}_6$ and $R_c$ are the effective coupling constant and blockade radius, respectively. The interaction (2) can be generated from the strong vdW interaction $C_6/r^6$ ($C_6 = 9.7 \times 10^{20}$ a.u.) between highly excited Rydberg atoms via off-resonance dressing [18]. Consequently, the interaction between two far-distant ground-state atoms is $U(\mathbf{r}-\mathbf{r}') \simeq \tilde{C}_6/r^6$, where $\tilde{C}_6 = \nu^2 C_6$ and $\nu = (\Omega/2\Delta)^2$, with $\Omega$ the Rabi frequency and $\Delta$ the laser detuning, respectively. At shorter distances, ground-state atoms enter the vdW blockade regime [19] to which the effective interaction saturates. The local interaction due to $s$-wave scattering is $g = 4\pi\hbar^2 a/M$, with $a$ the scattering length and $M$ the atomic mass. In the cylindrical coordinates $(\rho,\phi,z)$, the harmonic trapping potential $V_{\text{ext}}(\mathbf{r}) = (M\omega_\perp^2/2)(\rho^2 + \lambda^2 z^2)$, with $\omega_\perp$ the radius frequency and $\lambda$ the aspect ratio. The condensate wave function $\Psi$ is normalized under $N = \int |\Psi|^2 d\mathbf{r}$, with $N$ the number of ground-state atoms.

Choosing the blockade radius $R_c$ and $\tau \equiv R_c^2 M/\hbar$ as the length and time scales, Eq. (1) can be rewritten as

$$i\partial_t\psi(\mathbf{r},t) = \left[-\frac{\nabla^2}{2} + \frac{\omega^2(\rho^2 + \lambda^2 z^2)}{2} + \gamma|\psi(\mathbf{r},t)|^2 \right.$$
$$\left. + \alpha\int\frac{|\psi(\mathbf{r}',t)|^2 d\mathbf{r}'}{1 + |\mathbf{r}-\mathbf{r}'|^6}\right]\psi(\mathbf{r},t), \quad (3)$$

where we have redefined the normalized wave function $\psi \equiv \sqrt{R_c^3/N}\,\Psi$, the strength of the radius potential $\omega \equiv \omega_\perp\tau$, and the interaction constants $\gamma \equiv 4\pi N a/R_c$ and $\alpha \equiv MN\tilde{C}_6/\hbar^2 R_c^4$. To obtain ground-state wave functions, we computed the governing equation (3) with imaginary time propagation until the convergence of the normalized wave function with error less than $10^{-6}$. Moreover, we have used the method of lines with spatial discretization by the Fourier pseudospectral method. The time integration in Eq. (3) is done by the adaptive Runge-Kutta method of order 2 and 3, which is more time efficient due to an adjustable time step.

For the trapped Rydberg-dressed BEC, one can define useful characteristic lengths $a_\perp \equiv \sqrt{\hbar/M\omega_\perp}$ and $a_\parallel \equiv a_\perp/\lambda$, corresponding to the radial and axial potentials, respectively. The spectrum and the onset of instability are tunable by varying the particle number or the confining potential. By varying the two ratios $R_c/a_\perp = \sqrt{\omega}$ and $R_c/a_\parallel = \sqrt{\lambda\omega}$, one can effectively have quasi-1D ($\sqrt{\omega} \gg 1$ and $\sqrt{\lambda\omega} \approx 1$) or quasi-2D ($\sqrt{\omega} \approx 1$ and $\sqrt{\lambda\omega} \gg 1$) limits.
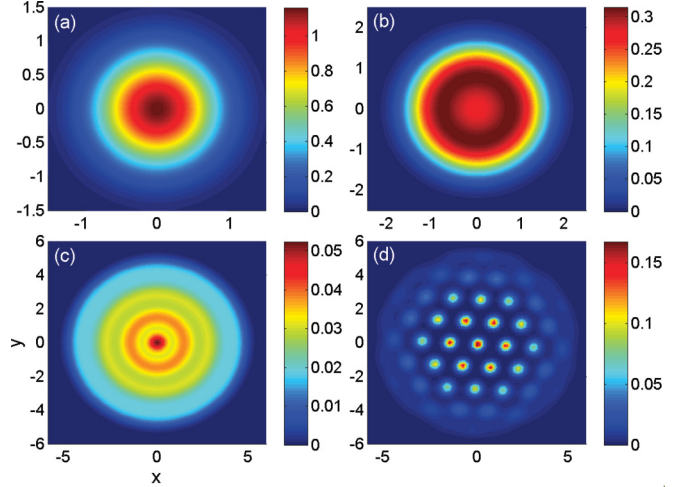


FIG. 1. (Color online) Density modulations of the quasi-2D Rydberg-dressed condensate with $\omega = 3$, $\lambda = 8$, $\gamma = 0$, and $\alpha = 10$ (a), 50 (b), 2000 (c), and 3000 (d). Case (c) corresponds to ringlike structures, while case (d) corresponds to the hexagonal crystal structure of BEC droplets. All axes are in units of $R_c$.

### A. Ground-state density profiles

The case of a quasi-2D geometry with $\omega = 3$ and $\lambda = 8$ is studied first. Figure 1 shows the condensate density profile varying with the strength of the dimensionless dressed interaction $\alpha$. When $\alpha$ is small, the ground-state density profile exhibits typical behaviors of a central peak [see Fig. 1(a)]. As $\alpha$ increases, the central density is too high to be stable and thus starts to modulate. Figure 1(b) shows a cratered condensate due to the central instability. As $\alpha$ increases further, owing to the roton instability occurring in the modulated density (see later), the condensate wrinkles violently and forms a ring structure [see Fig. 1(c)]. When $\alpha$ is increased above a critical value $\sim 2300$, the condensate eventually forms a droplet lattice. Figure 1(d) shows the quasi-2D Rydberg-dressed BEC forming a hexagonal droplet lattice with $\alpha = 3000$.

It is of particular importance and interest to examine whether the crystalline structure shown in Fig. 1(d) is actually experimentally accessible. The case of $\alpha = 3000$ can correspond to the following reasonable set of experimental parameters. One can consider ground-state $^{87}$Rb atoms coupled to excited Rydberg $nS$ state $^{87}$Rb atoms with $n = 60$ via a Rabi frequency $\Omega = 2\pi \times 2.2$ MHz and a red laser detuning $|\Delta| = 2\pi \times 75$ MHz. It will then admix a small fraction $\nu = (\Omega/2\Delta)^2 = 2.2 \times 10^{-4}$ of Rydberg character into the ground-state atoms with the blockade radius $R_c = (C_6/2\hbar|\Delta|)^{1/6} = 3.13$ $\mu$m [13]. In addition, the effective lifetime of dressed atoms $1/\gamma_{\text{eff}} = 1/\nu\gamma_r \sim 0.46$ s is as large as hundreds of milliseconds with the Rydberg state decaying rate $\gamma_r \sim 10$ ms$^{-1}$ [16]. Moreover, total number of ground-state atoms will be $N \sim 5 \times 10^3$, which corresponds to $N_r = \nu N \sim 1.1$ for the number of excited Rydberg atoms. By counting the number of droplets as $\sim 30$ in Fig. 1(d), an average of 0.037 excited Rydberg atom per droplet is found. This also justifies the validity of the GP treatment with the two-body dressing interaction $U(\mathbf{r}-\mathbf{r}')$ [20].

The formation of the ringlike structures [Fig. 1(c)] can be understood in the uniform limit $V_{\text{ext}} \to 0$. For a

uniform superfluid BEC with a density of $n_0 = 1/V$ (where $V$ denotes the volume), the corresponding excitation spectrum calculated from the Bogoliubov–de Gennes equations is a function of wave number $k = |\mathbf{k}|$ (in units of $1/R_c$): $\varepsilon(k) = \{k^2/2[k^2/2 + 2\alpha n_0 \tilde{U}(k)]\}^{1/2}$, where $\tilde{U}(k) = (2\pi^2/3)(e^{-k/2}/k)[e^{-k/2} - 2\sin(\pi/6 - \sqrt{3/4}k)]$ is the Fourier transformation of the scaled interaction $1/(1 + |\mathbf{r} - \mathbf{r}'|^6)$ in Eq. (3). The contact interaction $\gamma = 0$ is ignored in $\varepsilon(k)$. Including $\gamma$ will not affect roton instability when $\alpha$ is sufficiently large, nor will it affect the phonon behavior when $\alpha$ is small, to which the leading term of the expansion of $\tilde{U}(k)$ is a positive constant. That is, nonzero $\gamma$ modifies only the sound velocity. The excitation spectrum $\varepsilon(k)$ has asymptotically a phonon and a free-particle character at small and large $k$, respectively. However, with $\tilde{U}(k)$ having a negative minimum at some finite momentum, $\varepsilon(k)$ drops near that particular momentum and eventually becomes imaginary when increasing the strength $\alpha$. This suggests that the assumed uniform superfluid state is unstable toward the possible formation of nonuniform (periodic) order. Although the above $\varepsilon(k)$ is obtained for a uniform case, it is locally applicable to the condensate trapped in a slowly varying potential.

### B. Nonclassical rotational inertia fraction

To characterize the transition from concentric rings to a crystalline hexagonal lattice, we study the NCRIF, defined by $(I_0 - I)/I_0$. Here $I$ is the moment of inertia of the superfluid system under study and $I_0$ is its corresponding classical value [5]. As proposed by Leggett [4], the NCRIF of the superfluid system can be calculated in the limit of a small rotation. In the rotating frame, the free energy of a rotating BEC with rotation velocity $\omega_0$ about the $z$ axis is

$$F(\omega_0) = F_0 - \omega_0 \langle \psi, L_z \psi \rangle = \int \left[ \frac{|(\nabla - i\omega_0 \mathbf{e}_z \times \mathbf{r})\psi(\mathbf{r})|^2}{2} \right.$$
$$+ \frac{\omega^2(\rho^2 + \lambda^2 z^2)}{2}|\psi(\mathbf{r})|^2 - \frac{\omega_0^2 \rho^2}{2}|\psi(\mathbf{r})|^2$$
$$\left. + \frac{\alpha}{2}|\psi(\mathbf{r})|^2 \int \frac{|\psi(\mathbf{r}')|^2 d\mathbf{r}'}{1 + |\mathbf{r} - \mathbf{r}'|^6} \right] d\mathbf{r}, \quad (4)$$

where $L_z = -i(x\partial_y - y\partial_x)$ is the $z$-component angular momentum operator and $F_0 = F(\omega_0 = 0)$ is the free energy of the system without rotation. When $\omega_0 \ll 1$, $F(\omega_0)$ can be expanded as $F(\omega_0) = F_0(\psi_g) - I\omega_0^2/2$, with $\psi_g$, taken to be real, the ground state of $F_0$. Since the classical moment of inertia is given by $I_0 = \int \psi_g^2 \rho^2 d\mathbf{r}$, we obtain for $\omega_0 \ll 1$

$$\text{NCRIF} = \frac{\int [|(\nabla - i\omega_0 \mathbf{e}_z \times \mathbf{r})\bar{\psi}|^2 - (\nabla \psi_g)^2] d\mathbf{r}}{\omega_0^2 \int \psi_g^2 \rho^2 d\mathbf{r}}$$
$$= \frac{\int \psi_g^2 [\nabla S(\mathbf{r}) - \mathbf{e}_z \times \mathbf{r}]^2 d\mathbf{r}}{\int \psi_g^2 \rho^2 d\mathbf{r}}, \quad (5)$$

where $\bar{\psi} = |\bar{\psi}| \exp(i\omega_0 S)$ is the ground state of $F(\omega_0)$. In arriving at Eq. (5) we have assumed that $|\bar{\psi}| \simeq \psi_g$ for $\omega_0 \ll 1$. Note that while $\omega_0$ disappears in the second line of Eq. (5), $S$ does depend on $\omega_0$. As a consequence, the NCRIF can be obtained by computing Eq. (5) with the solved $\bar{\psi}$ and $\psi_g$. Figure 2(c) plots the calculated NCRIF as a function of the strength $\alpha$. Three different orders of small rotating
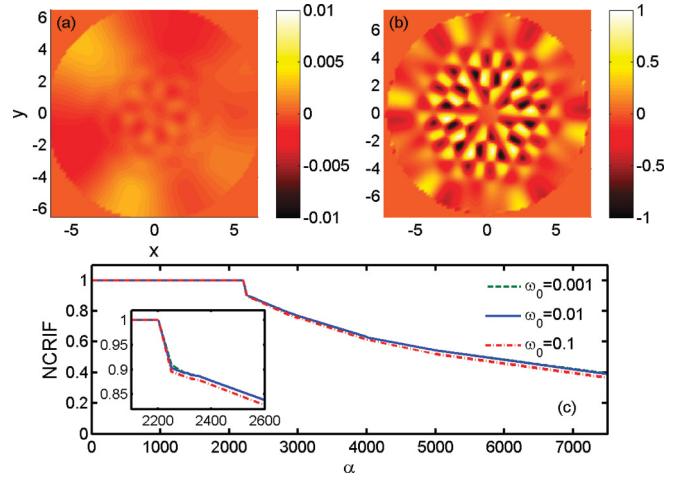


FIG. 2. (Color online) (a) and (b) Plots of $S(\mathbf{r})$, the local phase, divided by the rotation frequency $\omega_0$ for $\omega = 3$, $\lambda = 8$, $\gamma = 0$, $\omega_0 = 0.01$, and $\alpha = 2000$ (a) and 3000 (b). Phase modulation is much more stronger in case (b) than in case (a). (c) Plot of the calculated NCRIF [Eq. (5)], showing a drastic drop associated with the onset of the crystallization at $\alpha \sim 2300$ and the convergent behavior as $\omega_0 \to 0$.

frequencies, i.e., $\omega_0 = 0.1, 10^{-2}$, and $10^{-3}$, are taken and compared. One can see clearly that the curves are convergent when $\omega_0 \to 0$, which is anticipated for sensible results. There are two important factors revealed in the results of the NCRIF shown in Fig. 2(c). One is that the onset of the crystallization of BEC droplets is characterized by the drastic drop of the NCRIF, occurring at $\alpha = \alpha_c \sim 2300$. (No similar drop appears for the occurrence of a ringlike structure at smaller $\alpha$.) The other one is that while the NCRIF is reduced significantly when $\alpha > \alpha_c$, it remains a large value for a large span of $\alpha$. For example, $\mathcal{S}_{\text{NCRIF}} \geqslant 0.5$ for $\alpha \geqslant 6000$. This indicates that the superfluid (and hence the supersolid) is preserved within this regime.

To understand how the NCRIF drops drastically when a crystalized structure forms, in Figs. 2(a) and 2(b) we calculate and plot $S(\mathbf{r})$, the local phase, divided by the rotation frequency $\omega_0$. Figures 2(a) and 2(b) correspond to $\alpha = 2000$ (before crystallization) and 3000 (after crystallization), respectively, with the same rotation frequency $\omega_0 = 0.01$. One can see that $S$ modulates much more significantly in Fig. 2(b), about two order magnitude higher than in Fig. 2(a). This gives the key why the NCRIF drops drastically when a crystalized structure forms with $\alpha \geqslant \alpha_c$. Nonzero local phase modulation results in a nonzero local superfluid flow $\sim \psi_g^2 \omega_0 \nabla S$. When rotational symmetry is broken due to the formation of a crystalized structure, the ground state of the system must possess a nonzero superfluid flow to maintain the rigid-body rotation. This is the key why the phase modulation does not vanish as $\omega_0 \to 0$. This in turn results in the reduction of the nonclassical rotational inertia or the loss of the superfluid fraction. It is worth noting that while $S$ modulates significantly in Fig. 2(b), the magnitude of phase modulation $\omega_0 S$ is still small within the order of 0.01 [see Fig. 2(b)]. This again means that long-range superfluid phase coherence is preserved.

Superfluidity is usually strongly dependent on thermal and quantum fluctuations. As we are considering the limit of $T \to 0$, thermal fluctuation can be safely neglected. Moreover, as
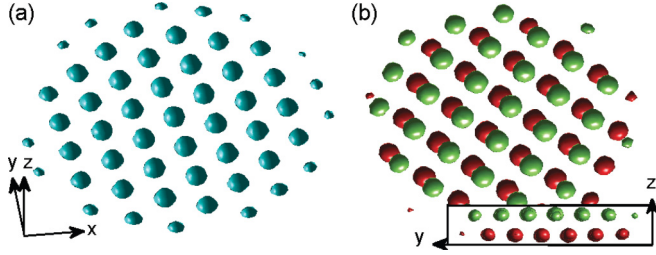
FIG. 3. (Color online) Comparison of (a) a monolayer and (b) a bilayer lattice structure: (a) the isosurface (isovalue 0.03) of the density with $\omega = 3$, $\lambda = 8$, $\gamma = 0$, and $\alpha = 5000$ and (b) the isosurface (isovalue 0.015) of the density with $\omega = 3$, $\lambda = 5$, $\gamma = 0$, and $\alpha = 10000$. The inset in (b) shows the bilayer being an $AB$ stack.

detailed in Sec. II A, the parameter regime under consideration is where the use of a two-body interaction is justified (i.e., there is no need to consider the three- or more-body interaction); the quantum fluctuation is typically small in this regime.

## III. MORE SUPERSOLID STRUCTURES

### A. Bilayers

By relaxing the originally frozen $z$-direction potential and/or increasing the particle number, the density starts to modulate in the $z$ direction and eventually forms a multilayer structure. Figures 3(a) and 3(b) compare the formations of a monolayer and a bilayer lattice. The inset in Fig. 3(b) indicates clearly that such a bilayer structure is an $AB$ stack.

### B. Anisotropy-induced square lattices

It is also interesting to note that when a Rydberg dressing interaction becomes anisotropic, the hexagonal lattice can shift to a nearly square lattice due to distortion of the interaction. This can occur when an external static electric field **E** is applied to the system (Stark effect) for which a two-photon mechanism will acquire an anisotropic component for the interaction, as compared to the purely isotropic case with **E** = 0 [21]. Figure 4 shows a nearly (though not perfectly) square lattice by using an interaction of the Heaviside-function form $\sim \theta(1 - \sqrt{x^2 + \kappa^2 y^2 + z^2})$ instead of $\sim 1/(r^6 + 1)$ as in Eq. (3). Here $\kappa$ corresponds to the anisotropic ratio. The static electric field is considered to be applied along the $y$ axis. Without losing generality, while the Heaviside-function interaction
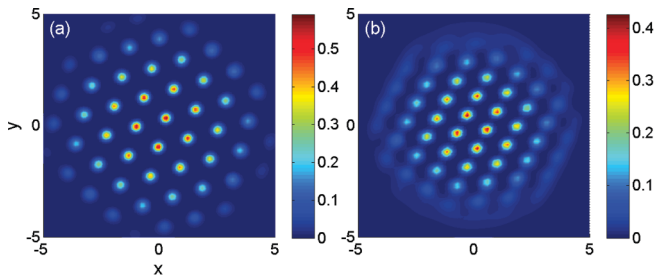


FIG. 4. (Color online) Comparison of (a) a hexagonal and (b) a nearly square lattice structure. The anisotropic ratio $\kappa$ of the interaction is (a) 1 and (b) 1.4 (see the text).
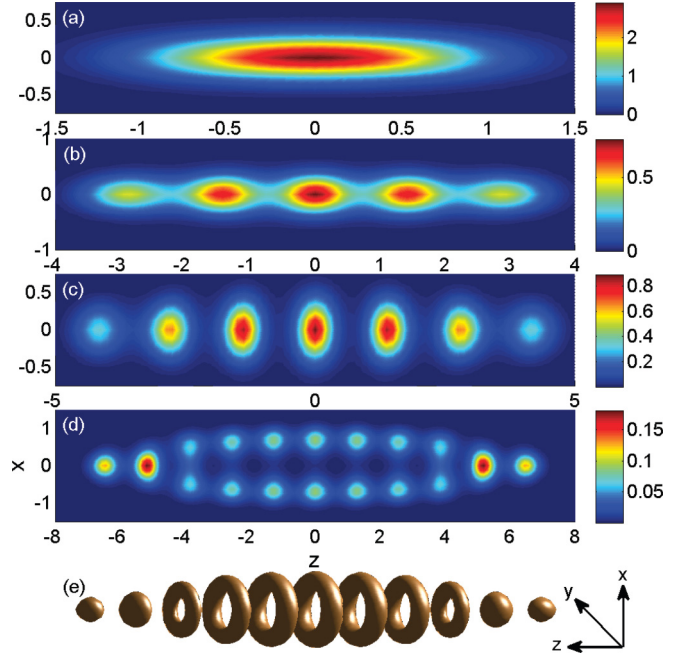


FIG. 5. (Color online) Density modulations of a quasi-1D condensate with $\omega = 15$, $\lambda = 0.2$, and $\alpha = 10$ (a), 250 (b), 500 (c), and 2000 (d). (e) shows the isosurface of modulation (d) with isovalue 0.05.

makes the simulation of anisotropy more convenient, it does capture a roton minimum in the excitation spectrum.

### C. Quasi-one-dimensional lattices

The condensate ground state in a quasi-1D system is also investigated with $\omega = 15$ and $\lambda = 0.2$. Figure 5 shows the modulation of the condensate density of a quasi-1D system by varying the strength of the dressing-induced interaction $\alpha$. When $\alpha$ is small, the system displays superfluidity and the density has a central peak [see Fig. 5(a)]. As $\alpha$ increases, the density starts to modulate and has multiple peaks. Figure 5(b) shows that there are five peaks in the condensate in the axial direction. With a sufficiently large $\alpha$, the condensate spontaneously crystallizes in the axial direction [see Fig. 5(c)]. As $\alpha$ increases further, the condensate starts to modulate in the frozen direction, forming a crystalline structure with a central hole [see Figs. 5(d) and 5(e)]. If $\alpha$ is extremely large, the condensate starts to cluster in the originally frozen direction and these clusters form a gyroidal chain.

## IV. CONCLUSION

In summary, based on the Gross-Pitaevskii treatment, spontaneously crystalline ground states, called quantum crystals, are numerically studied for a trapped Rydberg-dressed Bose-Einstein condensate. In a quasi-2D system, a hexagonal droplet lattice characterized by a drastic drop of the nonclassical rotational inertia is shown when the dressing interaction is sufficiently large. By relaxing the originally frozen axis, an $AB$ stacking bilayer lattice is observed. We also show that by applying a static electric field to make the interaction anisotropic, a nearly square droplet lattice can be obtained.

## ACKNOWLEDGMENTS

[1] O. Penrose and L. Onsager, Phys. Rev. **104**, 576 (1956).

[2] A. F. Andreev and I. M. Lifshitz, Sov. Phys. JETP **29**, 1107 (1969).

[3] G. V. Chester, Phys. Rev. A **2**, 256 (1970).

[4] A. J. Leggett, Phys. Rev. Lett. **25**, 1543 (1970).

[5] E. Kim and M. H. W. Chan, Nature (London) **427**, 225 (2004); Science **305**, 1921 (2004).

[6] M. Greiner, O. Mandel, T. Esskinger, T. W. Hänsch, and I. Bloch, Nature (London) **415**, 39 (2002).

[7] O. Morsch and M. Oberthaler, Rev. Mod. Phys. **78**, 179 (2006).

[8] K. Goral, L. Santos, and M. Lewenstein, Phys. Rev. Lett. **88**, 170406 (2002).

[9] T. Lahaye, C. Menotti, L. Santos, M. Lewenstein, and T. Pfau, Rep. Prog. Phys. **72**, 126401 (2009).

[10] G. Pupillo, A. Micheli, M. Boninsegni, I. Lesanovsky, and P. Zoller, Phys. Rev. Lett. **104**, 223002 (2010).

[11] F. Cinti, P. Jain, M. Boninsegni, A. Micheli, P. Zoller, and G. Pupillo, Phys. Rev. Lett. **105**, 135301 (2010).

[12] S. Saccani, S. Moroni, and M. Boninsegni, Phys. Rev. B **83**, 092506 (2011).

[13] N. Henkel, R. Nath, and T. Pohl, Phys. Rev. Lett. **104**, 195302 (2010).

[14] Y. Pomeau and S. Rica, Phys. Rev. Lett. **72**, 2426 (1994).

[15] X. Li, W. V. Liu, and C. Lin, Phys. Rev. A **83**, 021602(R) (2011).

[16] J. E. Johnson and S. L. Rolston, Phys. Rev. A **82**, 033412 (2010).

[17] F. Maucher, N. Henkel, M. Saffman, W. Królikowski, S. Skupin, and T. Pohl, Phys. Rev. Lett. **106**, 170401 (2011).

[18] K. Singer *et al.*, J. Phys. B **38**, S295 (2005).

[19] D. Jaksch, J. I. Cirac, P. Zoller, S. L. Rolston, R. Côté, and M. D. Lukin, Phys. Rev. Lett. **85**, 2208 (2000).

[20] J. Honer, H. Weimer, T. Pfau, and H. P. Büchler, Phys. Rev. Lett. **105**, 160404 (2010).

[21] A. V. Gorshkov, P. Rabl, G. Pupillo, A. Micheli, P. Zoller, M. D. Lukin, and H. P. Büchler, Phys. Rev. Lett. **101**, 073201 (2008).